Experimental flow characterization in a spiral vortex drop shaft

João Fernandes and Ricardo Jónatas

ABSTRACT

Connecting storm-sewers located at rather different elevations may be made with vortex drop shafts in which the energy dissipation is made by the friction between the vertical shaft and the flow and downstream by the impinging jet in a dissipation chamber. Following the first model design in the 1940s, different types of vortex drop shafts have been developed. One of the most used type is the so-called spiral vortex drop shaft developed to work in supercritical flow with good performance in both energy dissipation and space constrains. In this paper, an experimental flow characterization in a spiral vortex drop shaft is conducted covering the three main components of these structures, namely the inlet channel, the vertical shaft and the dissipation chamber. The results include measurement of water depths, pressure and velocity.

Key words | drop shaft, drop structures, energy dissipation, hydraulic model, vortex

João Fernandes (corresponding author)
Ricardo Jónatas
National Laboratory for Civil Engineering
Lisbon,
Portugal
E-mail: *jnfernandes@lnec.pt*

INTRODUCTION

The connections between storm-sewers located at different elevations are commonly made by plunge-flow inlet. For connections with considerably different elevations, vortex-flow inlet may be used with better performance in energy dissipation and safety due to more stable flow patterns (Zhao *et al.* 2006; Liu *et al.* 2018).

The first development of a vortex drop shaft is attributed to Drioli (1947) and was performed under subcritical approach flow. Since then, different configurations for intake structure of vortex drop shafts were developed. As presented in Figure 1, the selection of this component is mainly based on the approach flow and can be classified as circular, scroll, spiral or tangential (further details on these types of structures can be found in Jain & Ettema 1987). Its function is to guide the flow from the horizontal inlet pipe or channel to the vertical direction by creating a stable annular flow and ensuring appropriate air discharge to prevent pulsations and choking (Pfister *et al.* 2018).

Due to the 3 d flow mechanisms and the occurrence of air entrance, the flow across a drop structure is rather complex (Del Giudice & Gisonni 2011). Therefore, throughout the last decades some studies were devoted to the study of the flow characteristics and energy dissipation of these structures both experimentally and numerically.

Jain (1984) presents an experimental work to predict the hydraulic performance of a tangential vortex inlet obtaining a correlation between the drop shaft diameter and the discharge capacity. Following the work of Kellenberger (1988), Hager (1990) recommended the design of a spiral drop shaft in which the geometry depends mainly on the shaft radius and on the width of the inlet channel. The authors obtained similar discharge capacities of the vortex drop shafts for both sub- and supercritical approach flows. It was found that both the Froude number of the approach flow and the radius of outer inlet wall significantly influence the maximum height of the standing wave in the vortex structure.

Following a comprehensive experimental study, Yu & Lee (2009) characterized the flow mechanisms in a tangential vortex intake. It is shown that the hydraulic stability depends on the discharge at which flow control shifts from upstream to downstream. A general guideline for designing a tangential vortex intake that can convey the flow smoothly without unstable fluctuating flow associated with a hydraulic jump is presented.

Del Giudice *et al.* (2010) investigated changes to be made in the supercritical approach channel if a subcritical scroll vortex intake is used. The experimental investigation analyzes the effect of a hydraulic jump on the performance of vortex intake structure to define appropriate technical solutions.

Liu *et al.* (2018) improved the flow stabilization in an intake structure of a drop shaft with the inclusion of inlet swirling-flow-generating piers. The authors analysed by

doi: 10.2166/wst.2019.274

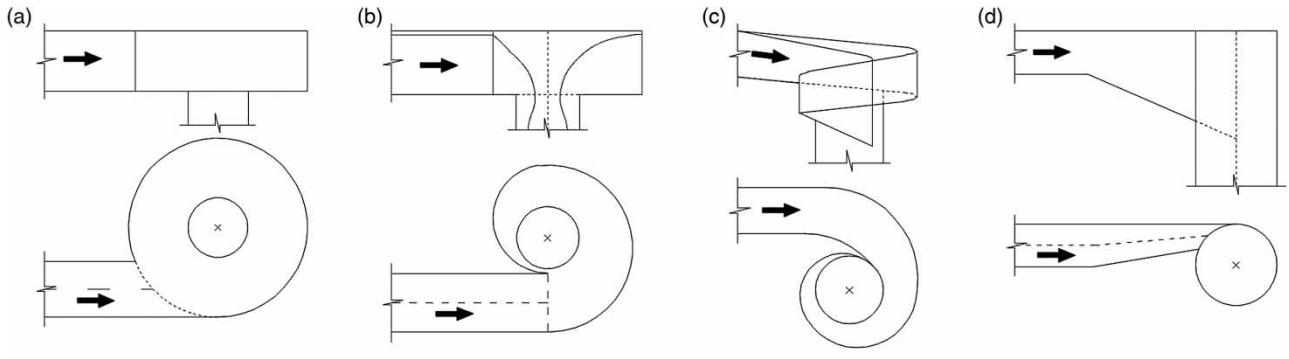

Figure 1 | Types of vortex drop shafts: (a) circular, (b) scroll, (c) spiral and (d) tangential.

means of numerical simulations the influence of the number of piers, pier weir angle, weir head, and pier height on the inlet's discharge coefficient. The authors reveal the rotational flow movement mechanism of the self-regulating swirl piers and the energy dissipation of the new structure and analytic calculations were proposed.

The performance of constructed vortex drop shafts was evaluated in several references (e.g. Kellenberger 1988). Echávez & Ruiz (2008) presented the flow characteristics of a spiral drop shaft after 35 years of operation. The authors reported a satisfactory hydraulic behavior of the structure. The difficulties in the construction due to the complex geometry were reported by Weiss *et al.* (2010). Due to delicate moulding work and the construction costs of spiral vortex drop shafts, a new vortex drop shaft with simplified geometry was preferred and constructed.

Pfister *et al.* (2018) presented a novel concept of vortex drop shaft that comprises a junction chamber to merge the inflow branches followed by a very short and steep inlet channel. An experimental study in a physical model proved the feasibility of this solution.

In the literature, a recent attention for vortex drop shafts is pointed out. Nevertheless, the recent advances were made in tangential drop shafts (Yu & Lee 2009; Liu *et al.* 2018), scroll drop shafts (Del Giudice *et al.* 2010) or in small adaptations of spiral drop shafts (Pfister *et al.* 2018). In this paper, an experimental work was developed to characterize the main hydraulic features in spiral drop shaft. A comprehensive understanding of the complete function of the structure is provided.

The current experimental study aims at enhancing the knowledge of the main flow mechanisms in spiral vortex drop shafts. Using state of the art equipment and physical modelling techniques, water depths, flow discharges, pressures and velocities were measured. Besides the flow characterization and its use for numerical modelling calibration or validation, this work intends to help engineers to design these structures.

EXPERIMENTAL FACILITY

The experimental campaign was conducted in a physical model of a spiral vortex drop shaft in the National Laboratory for Civil Engineering in Lisbon, Portugal. The complete structure comprises (i) an inlet channel, (ii) a vertical drop shaft, (iii) a dissipation chamber with an air venting pipe and (iv) an outlet pipe.

Whenever it was possible the model was constructed in transparent material (e.g. acrylic) to allow the visualization of the flow. Due to its complex geometry, the bottom of the vertical drop shaft was 3 d printed and later on implemented in the hydraulic model. A medium size reservoir in the upstream part of the facility ensures a constant head at the beginning of the inlet channel.

A global view of the model can be seen in the Supplementary Material (available with the online version of this paper).

The inlet channel connects the upstream constant-level reservoir and the intake structure. This channel is approximately 6 m long with a prismatic 0.216 m wide and 0.177 m height rectangular cross section and with a constant bottom slope, s_0, 0.01 m/m.

For each flow case, the reservoir is fed with a different flow discharge which features different levels that remains constant during each experiment (steady flow). In the transition from the reservoir to the inlet channel, the critical depth controls the supercritical flow in the inlet channel.

The intake structure is located downstream the inlet channel and assists the formation of the vortex transforming a rectilinear approach flow to a vertical shaft. The main geometrical characteristics were defined according the design recommendations of Kellenberger (1988) for a

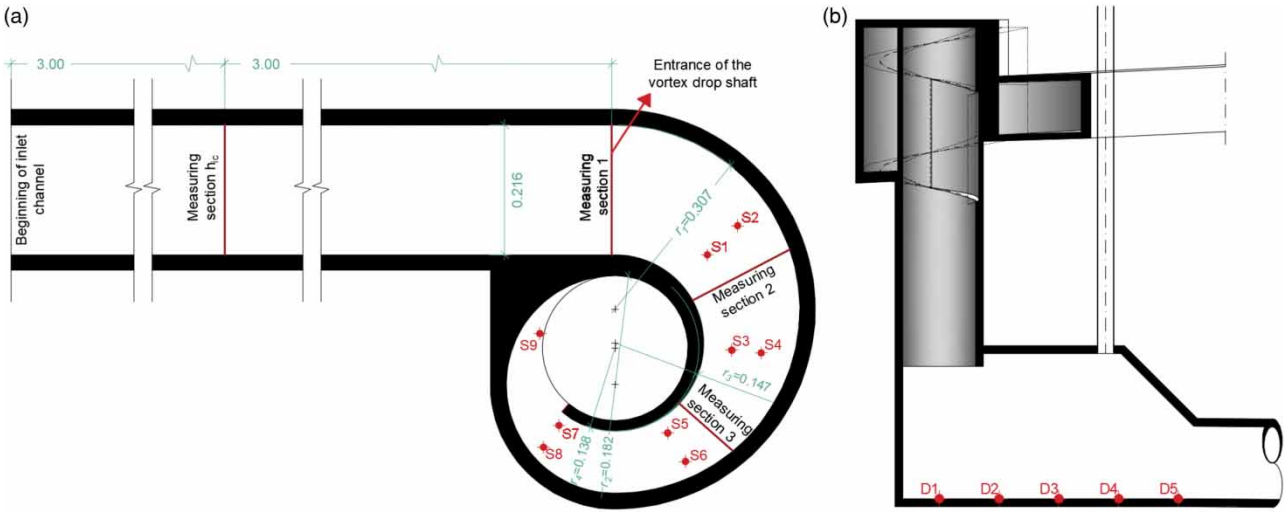

Figure 2 | (a) Top view of the drop shaft with the position of the velocity measurement sections 1 to 3 and pressure measurements (S1 to S9), values in m, and (b) general drawing of the structure and position of the pressure measurement in the dissipation chamber (D1 to D5).

supercritical approach flow. Therefore, the structure has a constant bottom slope, $s_{0i} = 0.20$ m/m and comprises three shaft radius, $r_1 = 0.307$ m, $r_2 = 0.182$ m, $r_3 = 0.147$ m and $r_4 = 0.138$ m as presented in Figure 2.

The vertical shaft has a diameter $d = 0.242$ m and a height equal to 1.1 m.

In the bottom of the vertical drop shaft, a dissipation chamber aims transforming the remaining excess energy into heat such that the downstream flow is subcritical without velocity concentrations (e.g. Hager 1999). This chamber is 0.30 m wide, 0.48 m height and 0.97 m long.

Downstream the dissipation chamber, the water flows into a 4-m long outlet pipe with circular cross section with a diameter $d = 0.242$ m and a bottom slope of 0.0075 m/m. In the end of the outlet pipe, the water flows freely into the drainage system.

FLOW CONDITIONS AND EQUIPMENT

The experimental campaign comprised six flow cases described in Table 1 where subscript *ic* stands for the inlet channel and *h* means the uniform flow depth. In this case, the water depth in the middle of the cross section of the inlet channel was considered. Froude number, $Fr = U/(gR)^{1/2}$, where U is the average velocity, R is the cross-section hydraulic radius and g is the gravity acceleration and Reynolds number, $\mathrm{Re} = 4UR/\nu$, where ν is the kinematic viscosity, are also presented in Table 1. All experiments were conducted in steady flow conditions.

Table 1 | Summary of flow conditions

Flow case	Q (L/s)	h_{ic} (m)	R_{ic} (m)	Fr_{ic}	Re_{ic}
F1	10.6	0.052	0.035	1.614	132,557
F2	21.6	0.079	0.046	1.895	231,101
F3	30.5	0.106	0.054	1.832	284,606
F4	32.4	0.112	0.055	1.821	294,370
F5	35.4	0.117	0.056	1.876	313,925
F6	40.8	0.177	0.067	1.314	286,184

The measurements for all flow cases include: (i) flow depths in the inlet channel; (ii) flow depths in the outer part of the vortex drop shaft; (iii) flow pressure in the intake structure; (iv) flow depths and flow pressures in the dissipation chamber; and (v) flow depths in the downstream pipe. For specific flow cases, the cross sectional flow depths and velocities in the drop shaft were also measured.

The flow discharge was measured with electromagnetic flowmeters (Krohne M640/16 with inner diameter of 350 mm) whose overall measurement error is less than 0.5%. The medium pressures along the flow boundary were measured in the several components of the structure with piezometers connected to a multi-tubular manometer with maximum reading error of 1 mm of water column.

The results of the flow depth near the walls were directly measured with image processing (i.e. scanning the flow depths from photographs). The maximum errors are assumed to be 1 mm, therefore much less than the water fluctuations.

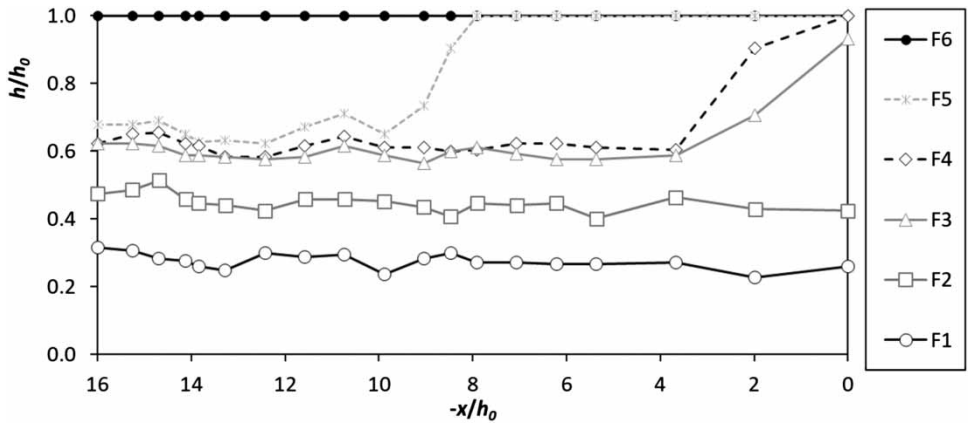

Figure 3 | Water depths in the inlet channel.

For specific flow cases, flow depths and velocities were measured within the vertical drop shaft area (see measurement cross sections 1 to 3 in Figure 3(a)). The flow depths were measured using ultrasonic level probes (Baumer UNDK 30) which use the emission of an acoustic sonic frequency of 240 kHz to determine its distance from a given surface reflector with a maximum error of 0.5 mm. In each point, the measurements were performed during 1 min with a frequency equal to 10 Hz. Flow velocities were measured using Ultrasonic Velocimetry probes (Monitor UVP-DUO) with a maximum resolution of 0.05 m/s and an accuracy of 0.8%.

For flow cases F1, F2, F4 and F6, the pressure was measured by means of piezometers in points S1 to S9 in the vortex structure and D1 to D5 in the bottom of the dissipation chamber.

RESULTS AND DISCUSSION

Inlet channel

For all experiments, supercritical flow was controlled by an upstream constant level reservoir (cf. Figure 1). Small disturbances were found in the water depths along the inlet channel. As these disturbances were attributed to small differences in roughness in the channel and were rather small (maximum differences in the longitudinal direction less than 5%), the flow was considered uniform and symmetrical in the inlet channel.

Figure 3 presents the water depths in the inlet channel. All values were non-dimensionalized with the inlet channel height, h_0. The reference of axis x corresponds to the longitudinal direction of the inlet channel with origin in the intake structure, i.e. section 1 in Figure 2.

Water elevations were measured in both sides of the inlet channel. Apart from flow case F4, as the results were similar, only the right side is presented.

Four distinct phenomena occur flow cases F1-F2, F3, F4-F5 and for F6.

For the first two flow cases, corresponding to the lower flow discharges, the flow depths in the inlet channel remain uniform (supercritical flow) until the entrance of the vortex drop shaft.

The flow seems to be controlled by the upstream condition and the influence of the intake structure is not felt.

For F3, the flow is influenced by the downstream intake structure, but the top of the inlet channel is not reached.

For the experiments featuring higher discharges, F4-F5, the discharge capacity of the intake structure affects the flow in the inlet channel. For F4, this hydraulic jump is rather asymmetrical with lower flow depth in the left side of the inlet channel (not shown here), corresponding to the inner side of the bend in the vortex drop shaft.

The discharge capacity for F6 in the vortex drop shaft was not enough to suitably convey the flow discharge. This lead to the pressurization of the whole inlet channel and a consequent increase of the water head in the upstream reservoir. For this flow discharge, the proposed design guidelines do not seem to be appropriate. Two possible solutions to obviate this problem are proposed to keep the current geometry (namely the diameter of the vertical shaft). Firstly, the increase of the slope of the inlet channel would lead to an increase of the flow velocity and to a reduction of the water depth. Secondly, the inlet channel height could be increased or eventually leave it open to the atmosphere.

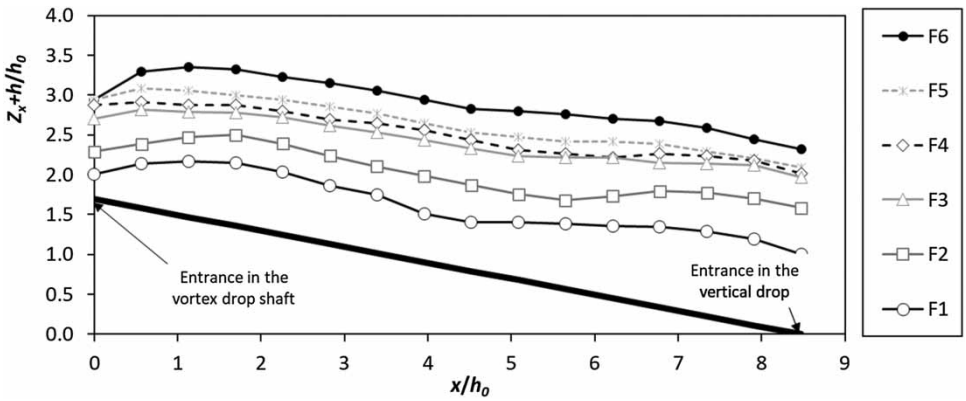

Figure 4 | Free surface in the outer guiding wall of the vortex drop shaft.

It should be pointed out that the functioning of flow cases F4-F6 should be avoided in real scale structures in order to allow for sufficient aeration of the flow in the vortex drop shaft (e.g. Hager 1985).

Vortex drop shaft

The free surfaces in the outer guiding wall of the vortex drop shaft for six flow cases are presented in Figure 4.

Water depths increase with the increase of the flow discharge. Figure 5 presents the results of the free surface and velocities measured in three cross sections (as presented in Figure 3) for flow cases F2 and F4. In the figures, y stands for the distance from the outer wall of the drop shaft in each cross section, linear quantities are non-dimensionalized by h_0, height of the inlet channel and velocities are non-dimensioanlized by the average velocity at the entrance of the vortex drop shaft, v_0.

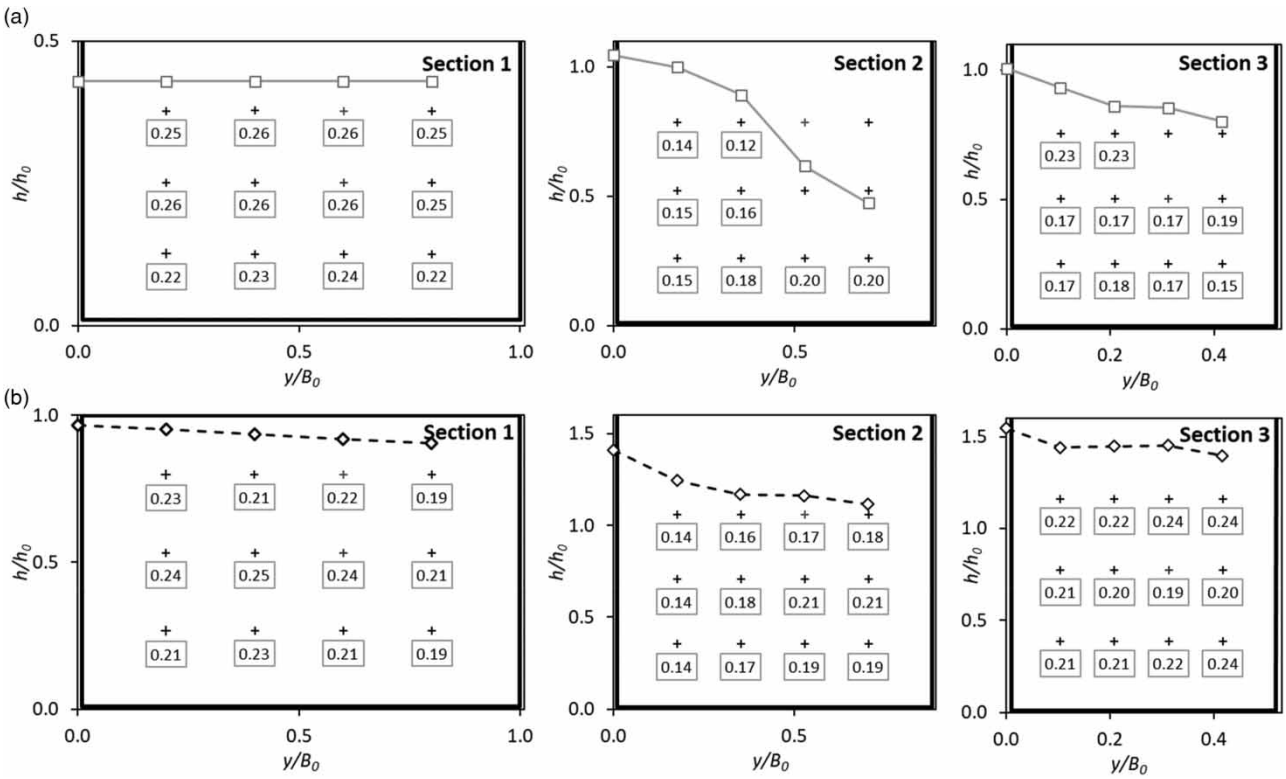

Figure 5 | Free surface and velocities in sections 1 to 3 for flow cases (a) F2 and (b) F4; non-dimensionalized velocities, v/v_0 are presented inside the boxes.

The results showed that a standing wave is identified along the outer guiding wall of the vortex drop shaft.

For flow cases F1, F2 and F3, corresponding to the lowest flow discharges, this wave features two maxima water depths which correspond to the typical pattern referred in the literature (e.g. Hager 1990). According to the experimental data analysed in Kellenberger (1988), the maximum flow depth with respect to the inlet section, h_m, may be given, according to the conditions in the inlet section, by the following equation:

$$\frac{h_m}{R_0} = (1.1 + 0.15Fr_0)\left[(2bh^2r_1^{-3})^{1/2}Fr_0 - \frac{s_v}{2}\right]$$

where b is the inlet channel width, h, R_0 and Fr_0 are the water depth, hydraulic radius and Froude number at the entrance of the vortex drop shaft and s_v is the slope in the vortex structure. For flow cases F1 to F4 the relative error obtained in the prediction of the maximum water depth varied between 4% and 9% whereas the error result for F5 is 13%. Due to the pressurized flow in the inlet channel, the result for F6 is erroneous with a relative error equal to 37%.

In the vertical shaft, an annular water flow was observed together with a central air cone. The cross sectional distribution of the free surface is presented in Figure 6 for flow cases F2 and F4. In the entrance of the vortex drop shaft, the free surface is completely flat for the case with lowest flow discharge. For F4, a small lateral slope is observed due to the influence of the downstream conditions. Due to the centrifugal force, the lateral slope of the free surface increases featuring a much higher flow depth in the outer guiding wall. This effect is much more marked for F2.

The velocity distribution in the inlet cross section is very uniform without a clear area with different velocity. In sections 2 and 3, the velocity increases in the inner part of the curve.

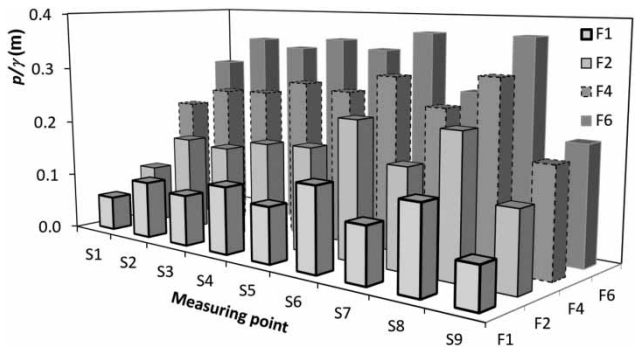

Figure 6 | Piezometric pressure measured in the vortex drop shaft bottom.

The average piezometric pressures were measured in the points indicated in Figure 3 for flow cases F1, F2, F4 and F6. The results are presented in Figure 6.

For the flow cases featuring higher flow discharges, the piezometric pressures are higher. For the same flow case, in the outer side of the vortex curvature, the pressure is higher ($p/\gamma_{S2} > p/\gamma_{S1}$ or $p/\gamma_{S4} > p/\gamma_{S3}$).

Dissipation chamber

The contact between the water and the vertical shaft walls contributes to the dissipation of energy whereas the dissipation chamber aims at dissipating the remaining flow energy.

The flow depth, non-dimensionalized by the chamber height, h_d, in the dissipation chamber is presented in Figure 7.

The vertical hollow jet impinges the bottom of the dissipation chamber leading to an air emulsion. The flow direction is rapidly changed from vertical to horizontal. It is a highly turbulent flow. The water surface increases as the flow discharge increases. It can be noted that the dimensions of the dissipation chamber seem to be adequate as the top of the chamber is not reached for the highest discharges. For all flow cases, the flow shows great aeration leading to an increase of the water depth. In Figure 7, the lines of the critical depth plus the intake loss in the transition were added in the outlet pipe. Even if the slope of the outlet pipe features a supercritical flow, due to the air entrainment, a higher flow depth is observed.

The pressure for flow cases F1, F2, F4 and F6 was measured in the bottom of the dissipation chamber in the positions presented in Figure 2. These results are presented in Figure 8.

The results show that higher pressure for flow cases featuring higher flow discharges. For flow case F1. Pressure remains approximately constant along the dissipation chamber, whereas for the other flow cases higher values are observed in the axis of the impinging jet coming from the vertical shaft. Following downstream the pressures are reduced at first and then increased due to the presence of the incline to the wall and to the entrance in the outlet pipe.

CONCLUSIONS

The connection between sewers at considerably different elevations may be made with vortex drop shafts. In these structures, the energy is reduced before the dissipation chamber due to the contact between the flow with the vertical shaft walls. Following the recent interest and the new

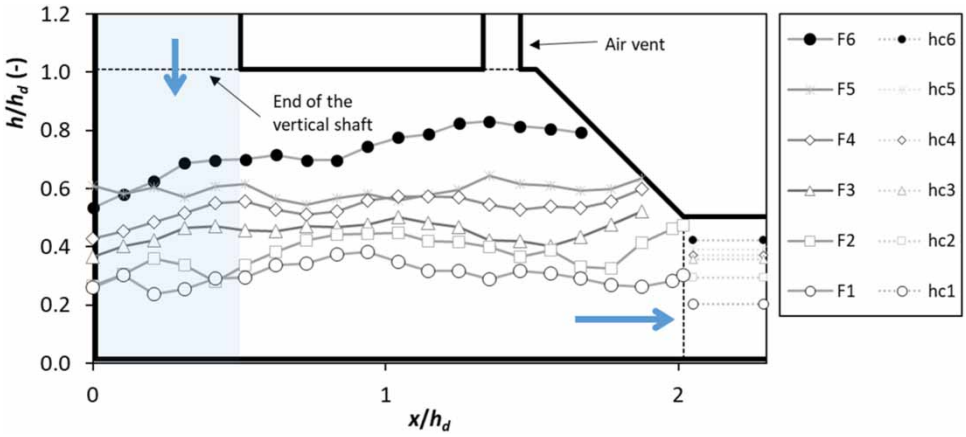

Figure 7 | Non-dimensionalized flow depth in the dissipation chamber, h/h_d.

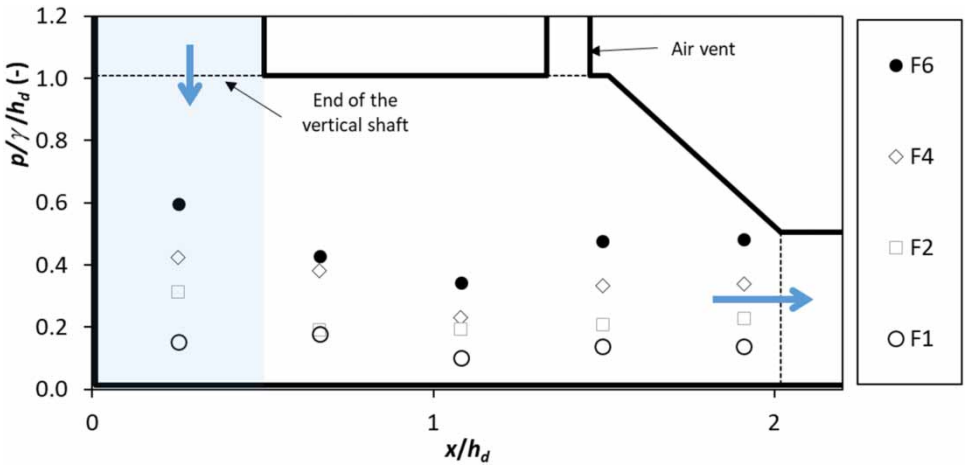

Figure 8 | Non-dimensionalized pressure in the dissipation chamber, p/γ.

project of such structures, this paper was devoted to an experimental characterization of the flow in a spiral vortex drop shaft. The experimental data can be used in the calibration and validation process of numerical modelling, as the main details regarding the structure are provided. Moreover, the results and conclusions are considered of interest not only for researchers but also for practitioners in the design procedure of such drop shafts.

For the six flow cases considered in the experimental campaign, different inlet conditions were obtained and in the entrance of the vortex drop shaft the flow was either subcritical or supercritical depending on the flow discharge. This different inlet conditions generated different conditions in the flow mechanisms and in the generation of a standing wave, as reported in previous studies.

The experimental results may help engineers to better design this type of structure and modelers to calibrate or validate their numerical simulations.

ACKNOWLEDGEMENTS

The first author acknowledges the support to Grant SFRH/BPD/114768/2016 and Project MixFluv – Mixing Layers in fluvial systems (PTDC/ECI-EGC/31771/2017) by FEDER and Science and Technology Foundation.

REFERENCES

Del Giudice, G. & Gisonni, C. 2011 Vortex drop shaft retrofitting: Case of Naples city (Italy). *Journal of Hydraulic Research* **49** (6), 804–808.

Del Giudice, G., Gisonni, C. & Rasulo, G. 2010 Design of a scroll vortex inlet for supercritical approach flow. *Journal of Hydraulic Engineering* **136** (10), 837–841.

Drioli, C. 1947 Su un particolare tipo d'imbocco per pozzi di scarico. *L'Energia Elettrica* **24**, 447–452 (in Italian).

Echávez, G. & Ruiz, G. 2008 High head drop shaft structure for small and large discharges. In: *Proceedings of the 11th*

International Conference on Urban Drainage, Edinburgh, Scotland, UK.

Hager, W. H. 1985 Head-discharge relation for vortex shaft. *Journal of Hydraulic Engineering* **111** (6), 1015–1020.

Hager, W. H. 1990 Vortex drop inlet for supercritical approaching flow. *Journal of Hydraulic Engineering* **116** (8), 1048–1054.

Hager, W. H. 1999 *Wastewater Hydraulics - Theory and Practice*. Springer-Verlag, Berlin and Heidelberg, Germany.

Jain, S. C. 1984 Tangential vortex-inlet. *Journal of Hydraulic Engineering* **110** (12), 1683–1699.

Jain, S. C. & Ettema, R. 1987 *Vortex-flow Intakes. IAHR Hydraulic Structures Design Manual*, Vol. 1. Balkema, Rotterdam, The Netherlands.

Kellenberger, M. H. 1988 *Wirbelfallschächte in der Kanalisationstechnik*. Doctoral dissertation, Swiss Federal Institute of Technology, Zurich, Switzerland (in German).

Liu, Z. P., Guo, X. L., Xia, Q. F., Fu, H., Wang, T. & Dong, X. L. 2018 Experimental and numerical investigation of flow in a newly developed vortex drop shaft spillway. *Journal of Hydraulic Engineering* **144**, 5.

Pfister, M., Crispino, G., Fuchsmann, T. & Ribi, J.-M. 2018 Multiple inflow branches at supercritical-type vortex drop shaft. *Journal of Hydraulic Engineering* **144**, 11.

Weiss, G., Brombach, H. & Hohl, E. 2010 Hydraulic model tests on a stormwater vortex drop shaft: Verification of special conditions. Novatech 2010.

Yu, D. Y. & Lee, J. H. 2009 Hydraulics of tangential vortex intake for urban drainage. *Journal of Hydraulic Engineering* **135** (3), 164–174.

Zhao, C. H., Zhu, D. Z., Sun, S. K. & Liu, Z. P. 2006 Experimental study of flow in a vortex drop shaft. *Journal of Hydraulic Engineering* **132** (1), 61–68.

First received 5 June 2019; accepted in revised form 30 July 2019. Available online 12 August 2019